Thermophoretically Dominated Aerosol Coagulation

Daniel E. Rosner[1,*] and Manuel Arias-Zugasti[2,1,†]

[1]*Chemical & Environmental Engineering Department, Yale University, New Haven, Connecticut 06520-8286, USA*
[2]*Departamento de Física Matemática y de Fluidos, UNED, Apdo: 60141, 28080 Madrid, Spain*

(Received 4 August 2010; published 6 January 2011)

A theory of aerosol coagulation due to size-dependent thermophoresis is presented. This previously overlooked effect is important when local temperature gradients are large, the sol population is composed of particles of much greater thermal conductivity than the carrier gas, with mean diameters much greater than the prevailing gas mean free path, and an adequate ''spread'' in sizes (as in metallurgical mists or fumes). We illustrate this via a population-balance analysis of the evolution of an initially log-normal distribution when this mechanism dominates ordinary Brownian diffusion.

DOI: 10.1103/PhysRevLett.106.015502 PACS numbers: 61.43.Hv, 05.20.−y

Normally, rate ''constants'' for fluid-phase physicochemical processes (such as homogeneous chemical reactions or suspended microparticle and/or droplet coagulation) in an isotropic carrier gas are scalar properties which depend on local state variables and *not* on their spatial gradients. However, in several studies it has been demonstrated that suspended particle thermophoresis (i.e., drift down a gas temperature gradient) can dominate Brownian diffusion as a transport mechanism—e.g., in the deposition of optical waveguide glass microdroplets [1–3], or the deposition of flame-generated particulate matter on heat exchanger surfaces [4]. This raises the interesting question of whether local conditions are met in applications in which aerosol coagulation rates are significantly altered in the presence of inevitable local temperature *gradients*. We investigate here when such effects should be expected and what the principal consequences will be. Remarkably, we demonstrate that this mechanism can locally dominate Brownian coagulation, e.g., for metallurgical mists and fumes—welding fumes, and, perhaps, aerosols produced in nuclear reactor coolant spills.

Our preliminary conclusions, summarized below, are based on a rational theory of aerosol particle coagulation resulting from size-dependent particle thermophoresis, when the underlying mechanism of particle phoresis outside of the free-molecule regime is the ''thermal creep'' boundary condition of ideal gas kinetic theory [5,6]. A dimensionless thermophoretic particle ''diffusivity,'' written here as $\tilde{\alpha} \equiv \alpha_T D_p/\nu$, may be defined by the vector expression for the particle drift velocity

$$\boldsymbol{V} = \tilde{\alpha}\nu(-\boldsymbol{\nabla}\ln T), \tag{1}$$

where T is the local carrier gas absolute temperature, ν the carrier gas momentum diffusivity, D_p the Brownian diffusion coefficient, and α_T (dimensionless) an effective thermal diffusion factor. For a spherical particle with intrinsic Fourier thermal conductivity k_p and diameter d_p the decisive factor $\tilde{\alpha}$ depends on particle size (via the Knudsen number based on gas mean free path ℓ and particle diameter $\mathrm{Kn} \equiv \ell/d_p$) and thermal conductivity ratio k_p/k_g (where k_g is the gas thermal conductivity), via the simple semiempirical relation [7] (plotted in Fig. 1)

$$\tilde{\alpha} = \frac{2C_s(k_g/k_p + 2C_t\mathrm{Kn})C}{(1 + 6C_m\mathrm{Kn})(1 + 2k_g/k_p + 4C_t\mathrm{Kn})}, \tag{2}$$

where C is the Cunningham-Millikan Stokes drag correction factor and approximate values of the remaining gas/solid interaction coefficients are given after Eqs. (2.21) and (2.56) of [8].

One notes immediately that, for any particular finite k_p/k_g ratio, the size-dependence of $\tilde{\alpha}$, the feature central to the coagulation mechanism considered here, peaks at intermediate Kn and vanishes in both the ''free-molecule'' and continuum limits. Inspection of the limiting value of $\tilde{\alpha}$ for $k_p/k_g \to \infty$, defined as $\tilde{\alpha}_\infty$, i.e.,

$$\tilde{\alpha}_\infty = \frac{4C_sC_t(1 + 2\mathrm{Kn}[A_1 + A_2e^{-A_3/\mathrm{Kn}}])\mathrm{Kn}}{(1 + 6C_m\mathrm{Kn})(1 + 4C_t\mathrm{Kn})} \tag{3}$$

reveals that in the limit $\mathrm{Kn} \to 0$, at most, $\tilde{\alpha} \sim \mathrm{Kn} \sim d_p^{-1}$ (locally).

A useful estimate of the collision rate ''constant'' (β_{12}) associated with differential thermophoretic drift of two particles of diameters d_1 and d_2 can be obtained by adapting Smoluchowski's estimate of the collision frequency

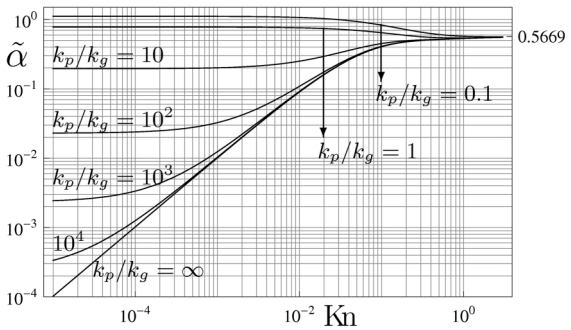

FIG. 1. Behavior of $\tilde{\alpha}$ [Eq. (2)] vs Kn.

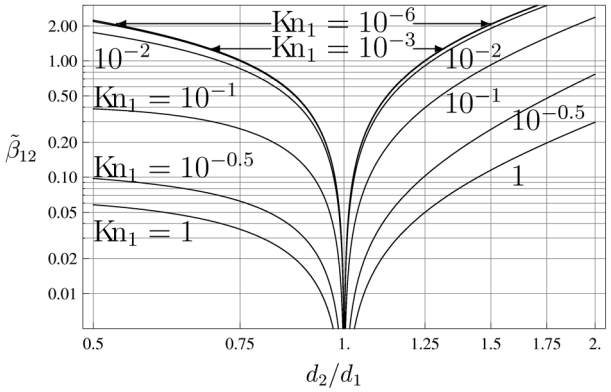

FIG. 2. Behavior of $\tilde{\beta}_{12}$ [Eq. (6)] vs d_2/d_1 for $k_p/k_g = 10^3$.

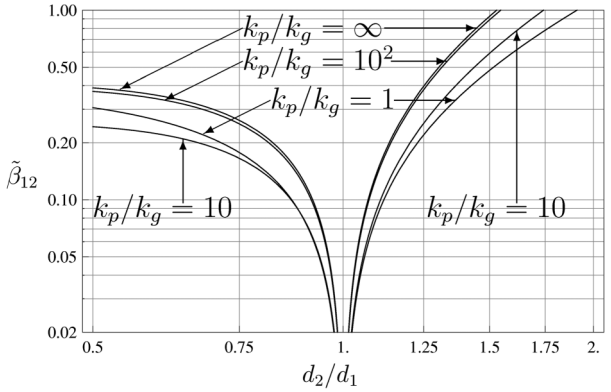

FIG. 3. Behavior of $\tilde{\beta}_{12}$ [Eq. (6)] vs d_2/d_1 for $\mathrm{Kn}_1 = 10^{-1}$.

for non-Brownian particles overtaking one another in a dilute suspension laminar shear flow, as summarized by Friedlander [8]. This method provides the simple symmetric result

$$\beta_{12} = (\pi/4)(d_1 + d_2)^2 \parallel \boldsymbol{V}_1 - \boldsymbol{V}_2 \parallel . \tag{4}$$

Combining Eqs. (2) and (4) leads us to define a nondimensional $\tilde{\beta}_{12} \equiv \beta_{12}/\beta_{\mathrm{ref}}$ where

$$\beta_{\mathrm{ref}} = (\pi/4) d_1^2 \tilde{\alpha}_{\infty,1} \nu \parallel \boldsymbol{\nabla} \ln T \parallel . \tag{5}$$

In these terms the dimensionless binary collision frequency can be expressed in the following compact form:

$$\tilde{\beta}_{12} = [1 + (d_2/d_1)]^2 |\tilde{\alpha}_1 - \tilde{\alpha}_2|/\tilde{\alpha}_{\infty,1} \tag{6}$$

which, for k_p/k_g and Kn in the range of maximum interest (see below) is not particularly sensitive to either parameter. Figures 2 and 3 show the interesting behavior of $\tilde{\beta}_{12}$, with features reminiscent of the dimensionless sedimentation kernel [8].

Before considering the consequences of this novel rate law when introduced into a Smoluchowski-type population balance for the evolution of a continuous number density distribution function $n(v, t)$ [with $v = (\pi/6) d_p^3$] we note that Brownian diffusion acting alone (e.g., in the absence of a temperature gradient) leads to the familiar rate constant $\beta_{B,12} = 2\pi(D_1 + D_2)(d_1 + d_2)$, where D_1 and D_2 are the corresponding Brownian diffusion coefficients (given by the slip-corrected Stokes-Einstein relation). Hence, thermophoretic coagulation will dominate Brownian coagulation when a Peclet number, defined as the ratio between typical thermophoretic and Brownian relative velocities, is much larger than 1

$$\mathrm{Pe} \equiv \frac{\parallel \boldsymbol{V}_1 - \boldsymbol{V}_2 \parallel}{2(D_1 + D_2)/(d_1 + d_2)} \gg 1. \tag{7}$$

Recalling the above-mentioned laws we find that the thermophoretic effect on aerosol coagulation will become dominant when, in addition to (C1) large local $\parallel \boldsymbol{\nabla} T \parallel$, the following somewhat less intuitive additional conditions are also met, viz.: the suspended particles have

(C2) much greater effective Fourier thermal conductivity than that of the carrier gas; i.e., $k_p/k_g > 10^2$.

(C3) mean diameters considerably larger than the prevailing gas mean free path; i.e., $\mathcal{O}(\mathrm{Kn}) < 10^{-2}$.

(C4) an adequate initial "spread" in diameters.

These expectations have been verified based on the predicted time evolution of initially log-normal continuous distributions of spherical particles, having specified the initial geometric standard deviation (σ_g) and Knudsen number (based on gaseous mean free path ℓ and Sauter mean diameter [8]), for k_p/k_g between 10 and ∞. Typical results are shown in Figs. 4 and 5, based on an efficient numerical solution of the Smoluchowski population-balance equation using a combined quadrature method of moments [9] along with orthogonal collocation [10]. These evolution simulations display the essential "fingerprints" of thermophoresis-driven coagulation, as discussed below.

One interesting result is that even though the coagulation rate β_{12} [Eq. (4)] is not a homogeneous function of particle

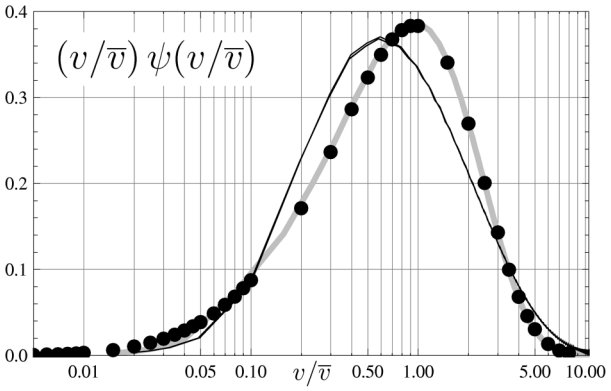

FIG. 4. Self-similar distribution function reached in the long-time limit for $k_p/k_g = 10$, 10^2, 10^3, 10^4, and ∞ (superimposed solid lines). Results for Brownian coagulation are also plotted for reference (gray line = present numerical scheme; solid dots after [19]—for aggregate fractal dimension = 3).

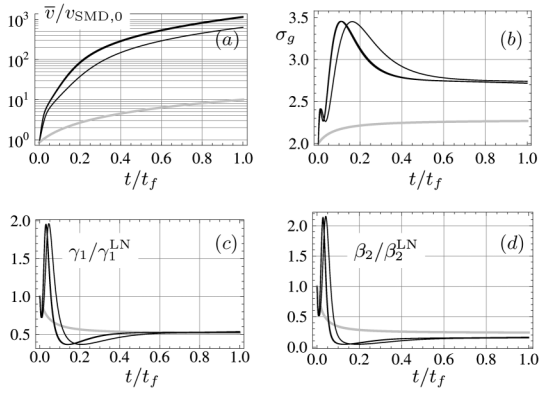

FIG. 5. Top: (a) average particle volume $\bar{v}$ over initial volume of a Sauter mean diameter particle $v_{\mathrm{SMD},0}$ and (b) geometric standard deviation σ_g of ψ vs stretched time. Bottom: (c) skewness γ_1 and (d) kurtosis β_2 of ψ over the corresponding results approximating ψ by a log-normal distribution; for $k_p/k_g = 10$ (separate solid line), 10^2, 10^3, 10^4, and ∞ (superimposed solid lines). Corresponding results for Brownian coagulation are also plotted for reference (gray lines).

volume, in the long-time limit the number density $n(v, t)$ approaches a self-similar distribution function $\psi(\eta)$ [8]; i.e., if we define a function $\psi(\eta, t)$ according to $n(v, t) \equiv N\psi(v/\bar{v}, t)/\bar{v}$ [where $\bar{v}(t)$ is the time-dependent average particle volume and $N(t)$ the total number density of particles], we find that in the long-time limit $\psi(v/\bar{v}, t)$ approaches a function that does not depend on time. The reason for this behavior is the following. As easily verified, once the population of particles reaches the low Knudsen number limit (d_1, $d_2 \gg \ell$); i.e., after a suitably long-time interval irrespective of the initial condition, the difference in thermophoretic velocity of two particles scales with

$$|\tilde{\alpha}_1 - \tilde{\alpha}_2| \simeq 4C_s \frac{\frac{C_t}{1+2k_g/k_p} + \frac{A_1-3C_m}{k_p/k_g}}{1 + 2k_g/k_p} \left| \frac{\ell}{d_1} - \frac{\ell}{d_2} \right|. \quad (8)$$

As a consequence, in that limit the dependence of the coagulation rate on particle size is given by

$$\beta_{12}|_{d_1,d_2\gg\ell} \propto (d_1 + d_2)^2 |(1/d_1) - (1/d_2)|. \quad (9)$$

Thus, when $\mathrm{Kn} \ll 1$, β_{12} becomes a homogeneous function of degree 1 in particle diameter (degree 1/3 in terms of particle volume). Because of the above-mentioned factorization of the β_{12} dependence on k_p/k_g and particle diameter, attained when $\mathrm{Kn} \ll 1$ for all particles in the population, we find that, in the long time limit, a population of particles under thermophoretically dominated coagulation will approach a ''self-preserving'' form (Fig. 4), independent of k_p/k_g. Also, because of factorization of the dependence on k_p/k_g and particle diameter of β_{12} reached once $\mathrm{Kn} \ll 1$, we find that the effect of k_p/k_g in the time evolution is merely to change the time scale (see Fig. 5). In Fig. 5 we show the average particle volume, along with the geometric standard deviation and the *symmetry* (skewness) and *flatness* (kurtosis) parameters of $\psi(v/\bar{v}, t)$ as a function of t/t_f, where t_f is the effective time needed to reach the self-preserving size distribution [$\psi(v/\bar{v})$], defined here as the time at which the time derivative of the 5 lowest order moments of ψ becomes smaller than 10^{-2}.

Our illustrative calculations suggest that the above-mentioned conditions are actually met in metallurgical mists and/or fumes, especially for high temperature operations carried out above atmospheric pressure (e.g., submerged gas jet refinement of molten metals or welding of offshore platforms, pipelines, etc.). However, even for micron-sized metal aerosols produced at ca. 1 atm pressure we find that the thermophoretic coagulation rate constant can exceed that for Brownian motion by a factor of 10. Turkdogan and Mills [11] reported condensation-enhanced diffusion-controlled evaporation rates (ca. threefold) of levitated, inductively heated Fe(L) + Ni(L) alloy droplets into 350 K He at $p = 1$ atm. Droplet diameters were ca. 0.64 cm and liquid surface temperatures were ca. 2300–2400 K. Thus, nominal temperature gradients were ca. 0.6×10^6 K/m, values comparable to those obtained locally in many combustion operations. In this case the (pressure-insensitive) k_p/k_g values were also probably of the order of 10^2. Thus, despite the fact that some Kn values probably exceeded unity, the presently estimated thermophoretically dominated coagulation rate constant for particles of, say, 0.3 and 3 μm is over 20 times that expected for Brownian diffusion acting alone. Moreover, a typical Peclet number of the type $V_p d_p/D_p$ (equal to the product of the particle thermal diffusion factor and relative change in temperature over one particle diameter) was of order 10^3. A slightly less extreme example is provided by the evaporation of molten sodium (e.g., nuclear reactor coolant) into argon [12]—a situation for which $\| \nabla T \| \sim 0.5 \times 10^5$ K/m, $k_p/k_g > 10^3$, and $V_p d_p/D_p$ probably exceeded 50 for particles estimated to be 1 μm diameter. The consequences of both mechanisms (Brownian diffusion and differential thermophoresis) acting together, i.e., when the Peclet number based on relative drift velocity, $(d_1 + d_2)/2$ and $D_1 + D_2$, is $\mathcal{O}(1)$ or less, will be the subject of a lengthier treatment, currently in progress.

On the face of it, the fact that we have shown that the local rate of aerosol coagulation, and the associated evolution of particle size distribution, in an isotropic gas mixture can be influenced by the presence of a local temperature *gradient* seems to violate a fundamental principle of the thermodynamics of linear irreversible processes (TIP), viz., a vectorial process should not be able to ''couple'' with a scalar process—a principle often ascribed to P. Curie [13,14]. However, one can view our present treatment as being outside the linear TIP domain since, as shown, it is the *magnitude* of the local vector ∇T that counts, irrespective of its direction. Put another way, if $\| \nabla T \|$ is viewed as $(\nabla T \cdot \nabla T)^{1/2}$ then we are, in effect, outside the realm of linearity. We are now dealing with a

more general nonlinear "constitutive law" for the coagulation rate, proportional to the "material frame-invariant" $\| \nabla T \|$, that all observers will be able to agree upon. On the other hand, even though at a molecular level the gas is an isotropic fluid, from the viewpoint of the suspended particles, i.e., at the "mesoscopic level," the gas is no longer isotropic because of the preferred direction defined by the local temperature gradient.

Last, we comment that particle coagulation in a local gaseous environment experiencing a large (volume-averaged) temperature gradient (treated here) should be distinguished from a previously studied case in which particle size-dependent radiation loss (or gain) causes temperature inequalities ($T_1 \neq T_2 \neq T_g$) in an otherwise uniform gas at temperature T_g [15]. In the latter case thermophoresis influences particle dynamics only when the coagulating particles enter each other's thermal "boundary layers"—i.e., those subregions occupying a volume at most comparable to the local volume fraction of suspended particles (often <1 ppm). Of course, in principle, both thermophoresis mechanisms could operate simultaneously, and both can become important under near-continuum conditions.

To summarize, we have identified conditions under which particle size-dependent thermophoresis can lead to significant increases in the coagulation rate constant and altered population dynamics of polydispersed aerosols composed of particles of the same Fourier thermal conductivity. We have shown that the thermophoretically dominated coagulation rate constant is proportional to the product of the magnitude of $\nabla \ln T$, the local carrier gas kinematic viscosity, the cross section $(\pi/4)(d_1 + d_2)^2$, and the difference in dimensionless thermophoretic diffusivities. We have also shown that when conditions $C1$–4 above are met, this mechanism can actually locally dominate Brownian coagulation—as in metallurgical mists and/or fumes [of interest in resource recovery, submerged jet refinement of metals, environmental control (welding fumes, etc.), or nuclear power plant accident analysis] or, perhaps, in "flame spray pyrolysis" (for the commercial aerosol synthesis of fine metal powders; see, e.g., [16]). Illustrative universal plots are provided to facilitate quantitative estimates in new situations and to display the "fingerprints" of this mechanism with regard to long-time size distribution-evolution. Generalizations are now required to account for short-range "hydrodynamic interactions," particle Brownian motion and shape effects, slow coalescence or sintering, nanoparticles in dense vapor carrier fluids, and other nonadditive combined coagulation mechanisms [14,17,18].

This exploratory study was supported by NSF under Grant No. CBET-1037733 to Yale University. M. A. Z. also gratefully acknowledges grants by Ministerio de Ciencia e Innovación (#ENE2008-06515-C04-03) and Comunidad de Madrid (#S2009/ENE-1597) at UNED.

*daniel.rosner@yale.edu
†maz@dfmf.uned.es

[1] K. L. Walker, G. M. Homsy, and F. T. Geyling, J. Colloid Interface Sci. **69**, 138 (1979).
[2] D. E. Rosner and S. S. Kim, Chem. Eng. J. (Lausanne) **29**, 147 (1984).
[3] D. E. Rosner and H. M. Park, Chem. Eng. Sci. **43**, 2689 (1988) [see Appendix 5; add missing exponent -1 to far right-hand side of Eq. (A5-1)].
[4] D. E. Rosner, *Transport Processes in Chemically Reacting Flow Systems* (Dover, Mineola, NY, 2000).
[5] S. Loyalka, Phys. Fluids A **1**, 403 (1989).
[6] D. E. Rosner and D. H. Papadopoulos, Ind. Eng. Chem. Res. **35**, 3210 (1996).
[7] L. Talbot, R. K. Cheng, R. W. Schefer, and D. R. Willis, J. Fluid Mech. **101**, 737 (1980).
[8] S. K. Friedlander, *Smoke, Dust and HazeFundamentals of Aerosol Dynamics* (Oxford University Press, Oxford U.K., 2000).
[9] R. McGraw, Aerosol Sci. Technol. **27**, 255 (1997).
[10] M. Arias-Zugasti, J. Aerosol Sci. **37**, 1356 (2006).
[11] E. T. Turkdogan and K. C. Mills, Trans. Metall. Soc. AIME **230**, 750 (1964).
[12] T. Kumada, R. Ishiguro, and F. Kasahara, J. Nucl. Sci. Technol. **15**, 912 (1978).
[13] S. R. de Groot and P. Mazur, *Non-Equilibrium Thermodynamics* (Dover, Mineola, NY, 1984), 2nd ed.
[14] D. E. Rosner and M. Arias-Zugasti, AIChE J. (in press).
[15] D. W. Mackowski, M. Tassopoulos, and D. E. Rosner, Aerosol Sci. Technol. **20**, 83 (1994).
[16] R. Grass and W. Stark, J. Nanopart. Res. **8**, 729 (2006).
[17] A. E. Ismail and M. Loewenberg, Phys. Rev. E **69**, 046307 (2004).
[18] H. Wang and R. H. Davis, J. Colloid Interface Sci. **159**, 108 (1993).
[19] S. Vemury and S. E. Pratsinis, J. Aerosol Sci. **26**, 175 (1995).